Inorg. Chem. **2003**, *42*, 1456–1461

Iron Hemiporphycene as a Functional Prosthetic Group for Myoglobin

Saburo Neya,*,† Kiyohiro Imai,‡ Hiroshi Hori,§ Haruto Ishikawa,|| Koichiro Ishimori,|| Daichi Okuno,⊥ Shigenori Nagatomo,⊥ Tyuji Hoshino,† Masayuki Hata,† and Noriaki Funasaki#

Department of Physical Chemistry, Graduate School of Pharmaceutical Sciences, Chiba University, Inage-Yayoi, Chiba 263-8522, Japan, Department of Nanobiology, Graduate School of Frontier Biosciences, Osaka University, Yamadaoka, Suita, Osaka 565-0871, Japan, Division of Biophysical Engineering, Graduate School of Engineering Science, Osaka University, Toyonaka, Osaka 560-8531, Japan, Department of Molecular Engineering, Graduate School of Engineering, Kyoto University, Kyoto 607-8501, Japan, Institute for Molecular Science, Okazaki National Institutes, Okazaki, Aichi 444-8585, Japan, and Department of Physical Chemistry, Kyoto Pharmaceutical University, Yamashina, Kyoto 607-8414, Japan

Received August 7, 2002

The iron complex of hemiporphycene, a molecular hybrid of porphyrin with porphycene, was incorporated into the apomyoglobin pocket to examine ligand binding ability of the iron atom in the novel porphyrinoid. Apomyoglobin was successfully coupled with a stoichiometric amount of ferric hemiporphycene to afford the reconstituted myoglobin equipped with the iron coordination structure of native protein. Cyanide, imidazole, and fluoride coordinated to the ferric protein with affinities comparable with those for native myoglobin. The ferrous myoglobin was functionally active to bind O_2 and CO reversibly at pH 7.4 and 20 °C. The O_2 affinity is 12-fold higher than that of native myoglobin while the CO affinity is slightly lower, suggesting decreased discrimination between O_2 and CO in the heme pocket. The functional anomaly was interpreted to reflect increased σ-bonding character in the Fe(II)–O_2 bond. In contrast with 6-coordinate native NO protein, the NO myoglobin containing ferrous hemiporphycene is in a mixed 5- and 6-coordinate state. This observation suggests that the in-plane configuration of the iron atom in hemiporphycene is destabilized by NO. Influence of the core deformation was also detected with both the infrared absorption for the ferrous CO derivative and electron paramagnetic resonance for ferric imidazole complex. Anomalies in the ferric and ferrous derivatives were ascribed to the modified iron–N(pyrrole) interactions in the asymmetric metallo core of hemiporphycene.

Introduction

Iron porphyrin distributes as the prosthetic group of hemoprotein in nature. The macrocycle is composed of four pyrrole rings connected with four *meso*-carbons. The fundamental structure is common over a wide range of natural and synthetic porphyrins. Recent advances in porphyrin synthesis allow us to manipulate the basic framework of porphyrin. The first example of a porphycene was discovered by Vogel et al.[1] in 1986. In remarkable contrast with the *meso*-carbon arrangement of (1,1,1,1) in porphyrin, the *meso*-carbons in porphycene are placed in a (2,0,2,0) manner. Core modification produces dramatic differences in the physicochemical properties of the parent porphyrin.[1,2]

Hemiporphycene is another notable example of the core-modified chromophore. As the name of "half-porphycene" denotes, hemiporphycene is a molecular hybrid of porphyrin with porphycene. It was first identified by Callot et al.[3] in 1995 on ring contraction of homoporphyrin and rationally synthesized by Vogel et al.[4] in 1997. In hemiporphycene,

* To whom correspondence should be addressed. E-mail: sneya@p.chiba-u.ac.jp. Tel: +81-43-290-2927. Fax: +81-43-290-2925.
† Chiba University.
‡ Graduate School of Frontier Biosciences, Osaka University.
§ Graduate School of Engineering Science, Osaka University.
|| Kyoto University.
⊥ Okazaki National Institutes.
Kyoto Pharmaceutical University.

(1) Vogel, E.; Köcher, M.; Schmickler, H.; Lex, J. *Angew. Chem., Int. Ed. Engl.* **1986**, *25*, 257−258.
(2) Vogel, E.; Balci, M.; Pramod, K.; Koch, P.; Lex, J.; Ermer, O. *Angew. Chem., Int. Ed. Engl.* **1987**, *26*, 928−931.
(3) Callot, H. J.; Rohrer, A.; Tschamber, T. *New J. Chem.* **1995**, *19*, 155−159.
(4) Vogel, E.; Bröring, M.; Weghorn, S. J.; Scholz, P.; Deponte, R.; Lex, J.; Schmickler, H.; Schaffner, K.; Braslavsky, S. E.; Müller, M.; Pörting, S.; Fowler, C. J.; Sessler, J. L. *Angew. Chem., Int. Ed. Engl.* **1997**, *36*, 1651−1654.

10.1021/ic020504t CCC: $25.00
Published on Web 01/30/2003

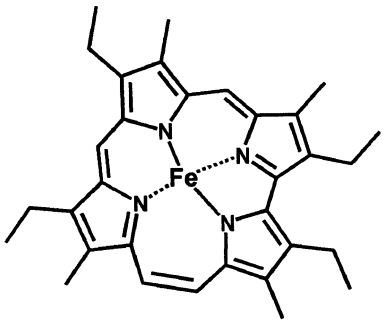

Figure 1. Structure of the iron hemiporphycene introduced into apoMb.

one *meso*-carbon atom is shifted to an adjacent *meso*-bridge so that the *meso*-carbons are placed in a (2,1,1,0) manner (Figure 1). The metallo cavity is asymmetric quadrate, imposing geometric strain on the chelating iron atom to induce possible reactivity changes toward the exogenous ligand.

Obvious structural similarity of hemiporphycene to porphyrin suggests possible utilization of iron hemiporphycene as a carrier of oxygen (O_2) and carbon monoxide (CO). It will be of primary concern to know the ligand binding ability of iron hemiporphycene, although such a successful attempt has not been so far reported. Stable oxygenation of ferrous hemiporphycene in hydrophilic environment is unlikely due to possible rapid autoxidation and formation of a μ-oxo dimer. For ferrous porphyrin, the undesirable side reactions can be suppressed with ingeniously designed derivatives.[5] In the case of simple iron hemiporphycene, reversible oxygenation under a physiological condition will be achieved only in hydrophobic environment. We consequently examined the coupling of iron hemiporphycene with protein matrix. We have previously reported that the iron complex of corrphycene,[6] an isomeric (2,1,1,0) porphyrin, can be introduced into myoglobin (Mb). This observation encouraged us to use apoMb as protein matrix for iron hemiporphycene; apoMb is indeed capable of accommodating the iron hemiporphycene to furnish stable holoprotein. We report the first detailed characterization of iron hemiporphycene in Mb. An account of the unique behaviors of the reconstituted Mb is provided on the basis of the peculiar molecular structure of the prosthetic group.

Experimental Section

Hemiporphycene and Iron Complex. 3,6,13,17-Tetraethyl-2,7,12,18-tetramethylhemiporphycene, or an etio-type of hemiporphycene (Figure 1), was used throughout the work. It was synthesized from ethyl 3,5-dimethyl-4-ethylpyrrole-2-carboxylate[7] according to the method of Vogel et al.[4] Anal. Calcd for $C_{32}H_{38}N_4$: C, 80.29; H, 8.00; N, 11.70. Found: C, 79.97; H, 7.98; N, 12.05. MS: *m*/*z* 478 (M^+). ^{1}H NMR (300 MHz, $CDCl_3$, δ): 10.09 (s, 1H, 15H), 9.81 (d, A part of an AB system, 1H, 9H), 9.77 (s, 1H, 20H), 9.74 (d, B part of and AB system, 1H, 10H, $J_{9,10}$ = 12.4 Hz), 4.18 (q, 2H, $-CH_2CH_3$), 4.02 (m, 6H, 3-CH_2-CH_3), 3.56, 3.51, 3.48, 3.46 (each s, 3H, $-CH_3$), 1.83, 1.81, 1.77, 1.71 (each t, 3H, $-CH_2CH_3$), -0.86 (br s, 1H, NH), -2.43 (br s, 1H, NH). Visible (dichloromethane) [λ_{max}, nm (ϵ_{mM})]: 404 (149), 480 (3.68), 510 (7.10), 551 (23.50), 581 (8.00), 631 (9.38). Iron was inserted to the macrocycle with the Adler method[8] to furnish ferric hemiporphycene chloride.

The ferrous pyridine hemochromogen spectrum was characterized to determine the reconstituted Mb. A minimum amount of aqueous sodium dithionite was added to ferric hemiporphycene dissolved in an equal volume mixture of pyridine/dimethylformamide. Visible [λ_{max}, nm (ϵ_{mM})]: 408 (92.4), 500 (11.7), 535 (11.3), 568 (sh, 29.2), and 575 (31.9).

Protein Reconstitution. Sperm whale Mb was purchased from Sigma (type II). Iron hemiporphycene was introduced into apoMb after the preparative method for etioheme-Mb.[9] Crude Mb was purified on a Whatman CM52-cellulose column in a cold room with a linear gradient of Tris/HCl buffer, 10−120 mM at pH 7.0. The yield of the Mb reconstitution was 70% or better.

Physical Measurements. The UV−visible absorption spectrum was recorded on a Shimadzu MPS-2000 spectrophotometer with a cell compartment connected with circulating water bath at 20 °C. The infrared (IR) spectrum of Mb, typically 0.1 and 2 mM, was obtained at 4-cm^{-1} resolution in the region of 1800−2200 cm^{-1} using a Jasco FT/IR-610 spectrometer attached with a cell of 26 μm light path length. Enriched ^{13}CO gas for the IR measurement of Mb^{13}CO was available from Icon Isotopes, NJ. The Electron paramagnetic resonance (EPR) spectrum was measured at X-band (9.226 GHz) microwave frequency on a Varian E12 EPR spectrometer with 100 kHz field modulation (0.5 mT). An Oxford flow cryostat (ESR-900) was used for measurements at liquid-helium temperature. Oxygen equilibrium curve was recorded with the automatic recording apparatus of Imai[10] in the presence of reducing enzyme system.[11] Equilibrium CO affinity was determined by titrating CO-saturated buffer to the MbO_2 solution in 0.1 M Tris at pH 7.0 and 20 °C.[12a] The association time course of CO or O_2 was obtained by a laser photolysis apparatus, Unisok USP-501. The absorption changes were monitored with a continuous probe light from a xenon lamp passed through a band-path filter (441 nm) and detected by a photo multiplier attached on a monochromator. A two-channel oscilloscope, Tektronix TDS-520, was used to digitize and accumulate the signals. The dissociation rate of O_2 was determined with a Unisok stopped-flow apparatus equipped with a rapid-scan monochromator, Olis RSM-1000, and that of CO was estimated from the equilibrium affinity and the association rate in 0.1 M Tris/HCl at pH 7.0 and 20 °C. Binding of solid ligands was spectrophotometrically monitored and analyzed with the Benesi−Hildebrand equation.[13] High affinity for cyanide was determined with the method of Brown.[14] The pK_3 value of hemiporphycene was measured with spectrophotometric pH titration.[9] Briefly,

(5) Momenteau, M.; Reed, C. A. *Chem. Rev.* **1994**, *94*, 659−698.
(6) (a) Neya, S.; Funasaki, N.; Hori, H.; Imai, K.; Nagatomo, S.; Iwase, T.; Yonetani, T. *Chem. Lett.* **1999**, 989−990. (b) Neya, S.; Nakamura, M.; Imai, K.; Funasaki, N. *Chem. Pharm. Bull.* **2001**, *49*, 345−346. (c) Neya, S.; Tsubaki, N.; Hori, H.; Yonetani, T.; Funasaki, N. *Inorg. Chem.* **2001**, *40*, 1220−1225.
(7) Johnson, A. W.; Markham, E.; Price, R.; Shaw, K. B. *J. Chem. Soc.* **1958**, 4254−4257.
(8) Adler, D.; Longo, F.; Kampas, F.; Kim, J. *J. Inorg. Nucl. Chem.* **1970**, *32*, 2443−2445.
(9) Neya, S.; Funasaki, N.; Imai, K. *Biochim. Biophys. Acta* **1989**, *996*, 226−235.
(10) Imai, K. *Methods Enzymol.* **1981**, *76*, 438−449.
(11) Hayashi, A.; Suzuki, T.; Shin, M. *Biochim. Biophys. Acta* **1973**, *310*, 309−316.
(12) Antonini, E.; Brunori, M. *Hemoglobin and Myoglobin in Their Reactions with Ligands*; North-Holland: Amsterdam, 1971; (a) pp 224−225, (b) pp 16−20, (c) pp 43−48.
(13) Benesi, H. A.; Hildebrand, J. H. *J. Am. Chem. Soc.* **1949**, *71*, 2703−2707.
(14) Brown, K. L. *Inorg. Chim. Acta* **1979**, *37*, L513−L516.

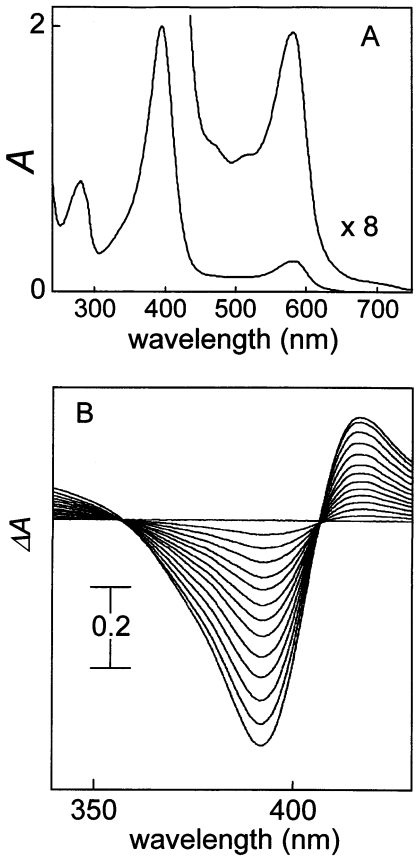

Figure 2. Electronic absorption spectra: (A) ferric Mb reconstituted with hemiporphycene in 0.1 M Tris at pH 7.0 and 20 °C with the Soret peak 2.5-fold higher than the 280-nm protein band; (B) acid−alkaline transition of ferric Mb with pK = 8.23 ± 0.17. The pH changed from 7.12 to 7.28, 7.47, 7.62, 7.80, 7.90, 8.02, 8.13, 8.23, 8.36, 8.50, 8.67, 8.87, and 9.15 in 10 mM Tris at 20 °C. The protein concentration is 14 μM.

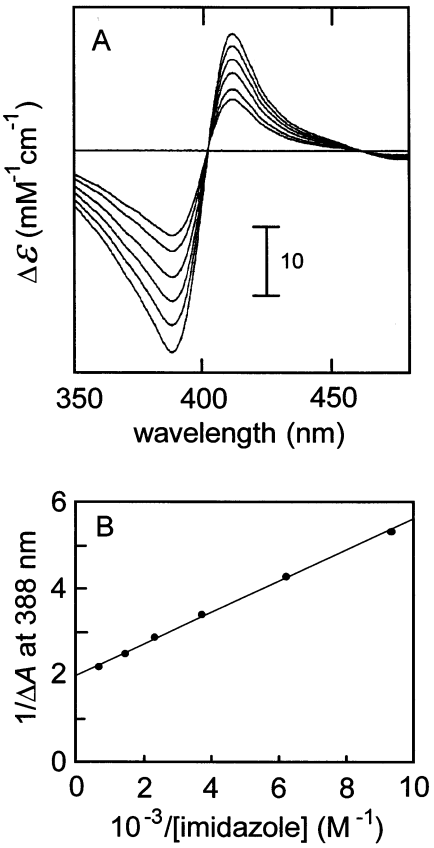

Figure 3. Imidazole binding to the Mb containing ferric hemiporphycene. The absorption change accompanied with isosbestic points at 405 and 472 nm afforded a binding constant $K = (5.43 \pm 0.27) \times 10^3$ M^{-1} for 13 μM Mb in 0.1 M Tris at pH 7.0 and 20 °C.

hemiporphycene dissolved in sulfuric acid was dropwise added to aqueous 2.5% sodium dodecyl sulfate, and the resultant homogeneous solution was adjusted to pH 10 with sodium hydroxide. Small increments of hydrochloric acid were added to the solution before visible absorption changes were recorded.

Results

Iron Hemiporphycene. Before accounting for the Mb reconstituted with iron hemiporphycene, the prosthetic group itself was first characterized. We evaluated the pK_3 value, a measure of basicity for the central nitrogens[15] of the free base. The pH titration of hemiporphycene in 2.5% sodium dodecyl sulfate solution with hydrochloric acid caused absorption decrease at 500 nm with well-defined isosbestic points at 529 and 560 nm (results not shown). Analysis of the absorption decrease with the Henderson−Hasselbalch equation, pK = pH + log([acid form]/[alkaline form]), afforded a pK_3 = 6.70 ± 0.21. The value is comparable with pK_3 = 6.38 of etioporphyrin.[9]

The electronic absorption spectrum of hemiporphycene ferric chloride in dichloromethane showed absorption maxima at 387 (117 mM^{-1} cm^{-1}), 480 (6.0), 568 (8.5), and 650 (3.9) nm. Imidazole titration to hemiporphycene ferric chloride in chloroform caused the Soret band to increase with isosbestic points at 397 and 460 nm (results not shown). Analysis of the 409-nm changes afforded a binding constant (4.37 ± 0.36) × 10^7 M^{-2}. The bis(imidazole) adduct in dichloromethane has absorption maxima at 406 (102 mM^{-1} cm^{-1}), 510 (5.7), 574 (14.1), and 700 (0.7) nm.

Ferric Mb. Optical titration of apoMb with ferric hemiporphycene revealed an inflection point at a 1:1 stoichiometry. Figure 2 shows the electronic absorption spectrum of the purified ferric Mb in purplish brown. The globin peak and Soret band are located at 280 and 396 nm, respectively; the absorbance ratio A_{396}/A_{280} = 2.5 is constant for several preparations. The extinction coefficient of the 396-nm Soret peak of ferric Mb at pH 7.0 was determined to be ϵ = 117 mM^{-1} cm^{-1} on the basis of the pyridine−hemochromogen spectrum described in the Experimental Section. The Soret absorption is markedly pH-dependent as shown in Figure 2; the transition can be fitted with a single-proton equilibrium with a midpoint at pH = 8.23 ± 0.17. Figure 3 shows the imidazole titration to the Mb which exhibited a binding constant $K = (5.43 \pm 0.27) \times 10^3$ M^{-1}. The visible spectrum of the imidazole derivative closely matches with that of the model compound, the bis(imidazole) complex of ferric hemiporphycene, as described in the foregoing section. Fluoride and cyanide coordinate with $K = 71 \pm 3$ M^{-1} and (5.9 ± 0.1) × 10^6 M^{-1}, respectively. The visible spectra of the ferric Mb derivatives are summarized in Table 1.

Figure 4 shows EPR spectra of the reconstituted Mb and related model compound. In the absence of exogenous ligand, ferric Mb shows high-spin signals at g = 6.71, 5.14, and 1.96_5 as well as a hemichrome type of low-spin signals at g

(15) Caughey, W. S. In *Inorganic Chemistry*; Eichhorn, G. L., Ed.; Elsevier: New York, 1973; Vol. 2, pp 797−831.

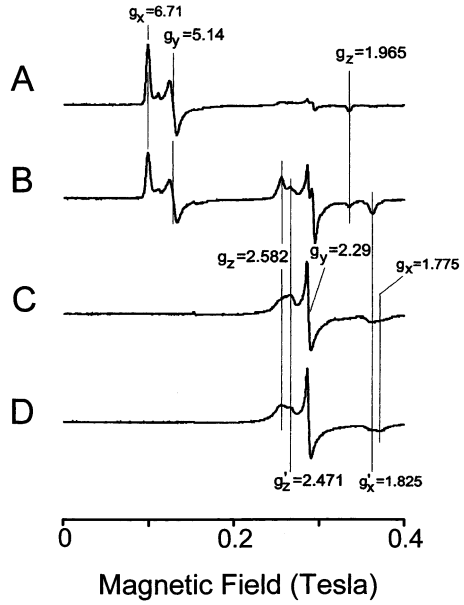

Figure 4. EPR of the ferric hemiporphycene and reconstituted Mb: (A) aquomet Mb, MbH_2O, in 0.1 M Tris/HCl at pH 7.0 and 5 K; (B) hemichrome partially formed in aquomet Mb at 15 K; (C) imidazole metMb in 0.1 M Tris/HCl at pH 7.0 and 15 K; (D) bis(imidazole) complex of ferric hemiporphycene in chloroform at 15 K.

Table 1. Visible Absorption Spectra of Mb Reconstituted with Iron Hemiporphycene in 0.1 M Tris/HCl at pH 7.0 and 20 °C

ligand	λ_{max}, nm (ϵ, mM^{-1} cm^{-1})				
	Ferric Derivatives				
H_2O	396 (102.0)	475 (6.9)	510 (6.5)	582 (12.3)	700 (0.4)
F^-	392 (90.0)	462 (10.3)	502 (8.4)	565 (12.2)	580 (12.5)
imidazole	403 (99.0)	510 (5.5)	571 (11.8)	700 (0.3)	
CN^-	407 (100.2)	510 (5.9)	550 (9.2)	572 (11.4)	710 (0.2)
	Ferrous Derivatives				
deoxy	423 (97.9)	470 (5.2)	560 (9.0)	598 (23.6)	
O_2	403 (92.5)	560 (10.0)	588 (12.8)		
CO	404 (117.3)	500 (9.9)	540 (8.0)	590 (6.8)	

= 2.58, 2.3, and 1.82 at 5 and 15 K (Figure 4, parts A and B). The latter signals disappeared on adding sodium fluoride to leave high-spin signals at g = 6.78, 5.18, and 1.97_4 (spectrum not shown). The split $g_\perp = 6$ signals for ferric Mb and the fluoride complex are consistent with lower molecular symmetry of the prosthetic group. The imidazole complex resolved two sets of the low-spin signals at g = 2.582, 2.29, and 1.775 and at g = 2.471, 2.29, and 1.825 with nearly comparable intensities. The EPR spectrum of imidazole Mb closely resembles that of ferric hemiporphycene bis(imidazole) complex in dichloromethane as illustrated in parts C and D of Figure 4.

Ferrous Mb. The ferrous deoxy Mb is functionally active to bind O_2 and CO reversibly. The visible absorption spectra of the deoxy, O_2, and CO derivatives are provided in Figure 5 and Table 1. The CO complex exhibits a Soret band and three visible maxima at 500, 540, and 590 nm. The spectral profiles of O_2 and deoxy derivatives are characteristic and dissimilar to those for native Mb derivatives.[12b] Figure 5 includes the Hill plots of O_2 binding with a Hill coefficient n = 0.97 and a half-saturating pressure P_{50} = 0.042 mmHg or $K_{O_2} = 1.3 \times 10^7$ M^{-1}. There is a ~10-fold increase in O_2 affinity when compared with etioheme-Mb[9] ($K_{O_2} = 0.9 \times 10^6$ M^{-1}) and mesoheme-Mb[16] ($K_{O_2} = 1.4 \times 10^6$ M^{-1}). On treatment of hemiporphycene-bound MbO_2 solution with CO-

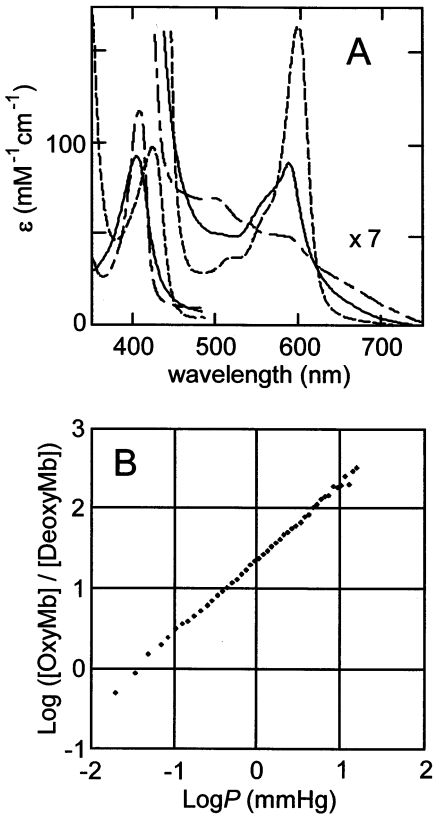

Figure 5. Ligand binding to the Mb containing ferrous hemiporphycene: (A) visible absorption spectra of the deoxy (---), O_2 (—), and CO (— · —) derivatives in 0.1 M Tris/HCl at pH 7.0 and 20 °C; (B) Hill plots of oxygenation of deoxy Mb in 0.1 M phosphate at pH 7.4 and 20 °C. Slope n = 0.97 and O_2 pressure at a half-saturation P_{50} = 0.042 mmHg were obtained.

saturated 0.1 M Tris buffer at pH 7.4 and 20 °C, a new Soret band developed with isosbestic points at 394 and 416 nm. From the Soret absorption changes, a partition coefficient $[MbCO][O_2]/[MbO_2][CO] = 1.70$ was obtained, corresponding to P_{50} = 0.033 mmHg or $K_{CO} = 2.2 \times 10^7$ M^{-1}. The CO affinity is comparable with or lower than those of mesoheme-Mb[16] ($K_{CO} = 2.1 \times 10^7$ M^{-1}) and native Mb[17] ($K_{CO} = 2.7 \times 10^7$ M^{-1}). The O_2 and CO ligation kinetics revealed that the association and dissociation rates are $k_{on} = (9.50 \pm 0.19) \times 10^6$ M^{-1} s^{-1} and $k_{off} = 1.72 \pm 0.03$ s^{-1} for O_2 and $k_{on} = (0.28 \pm 0.02) \times 10^6$ M^{-1} s^{-1} and $k_{off} = 0.013 \pm 0.010$ s^{-1} for CO, both in 0.1 M Tris/HCl at pH 7 and 20 °C. The $k_{off} = 1.7$ s^{-1} for O_2 is 1 order of magnitude smaller than $k_{off} = 15$ s^{-1} for native Mb.[17] The O_2 association rates are comparable between native and reconstituted Mbs. In contrast with the results of O_2 binding, the kinetic profiles of CO binding differed only slightly between native[17] and reconstituted Mbs.

The iron-bound CO probes the coordination environment of hemoprotein.[18] The IR spectrum of the coordinating CO in iron−hemiporphycene Mb exhibits three bands at 1928 (58%), 1942 (23%), and 1958 (19%) cm^{-1}, as shown in Figure 6. These bands are assigned to the iron-bound ^{12}CO

(16) Sono, M.; Smith, P. D.; McCray, J. A.; Asakura, T. *J. Biol. Chem.* **1976**, *251*, 1418−1426.
(17) Springer, B. A.; Sliger, S. G.; Olson, J. S.; Phillips, G. N., Jr. *Chem. Rev.* **1994**, *94*, 699−714.
(18) Maxwell, J. C.; Caughey, W. S. *Methods Enzymol.* **1978**, *54*, 302−323.

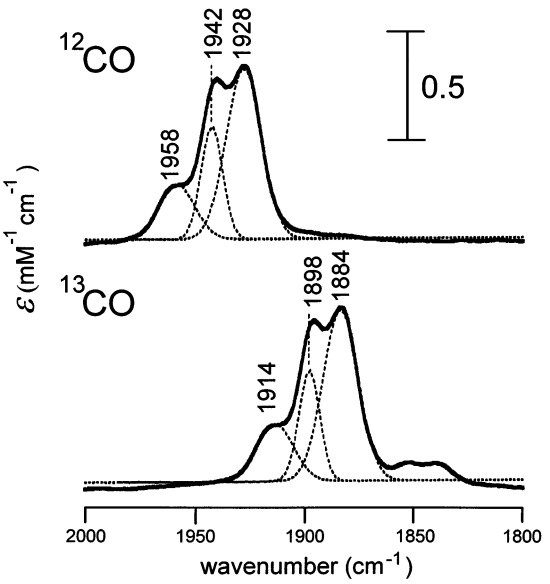

Figure 6. IR spectra of the MbCO reconstituted with ferrous hemiporphycene: (top) Mb^{12}CO; (bottom) Mb^{13}CO. Protein concentration is 2.2 mM in 0.1 M Tris/HCl at pH 7.0 and 20 °C.

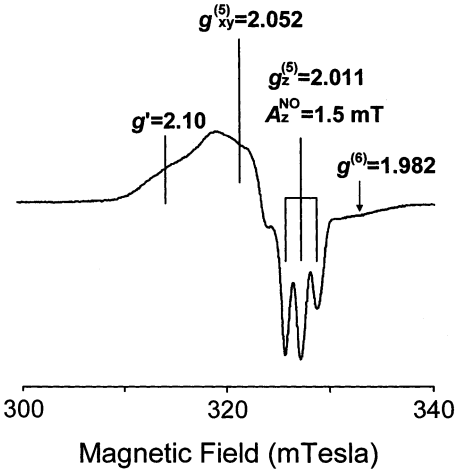

Figure 7. EPR spectrum of the Mb^{14}NO reconstituted with ferrous hemiporphycene. Protein concentration is 1.2 mM in 0.1 M Tris/HCl at pH 7.0 and 35 K.

since ligand replacement with ^{13}CO caused uniform shift to 1884, 1898, and 1914 cm^{-1} keeping almost the same pattern. The IR spectrum is in contrast with that of native Mb[19] showing two major peaks at 1945 (70%) and 1932 (30%) cm^{-1}.

The EPR spectrum of Mb^{14}NO at 35 K is illustrated in Figure 7. The major EPR signal exhibits a $g_{xy} = 2.052$ signal and a three-lined hyperfine splitting pattern ($A_z = 1.5$ mT) at $g_z = 2.011$. The spectral pattern is characteristic of a 5-coordinated NO-binding structure, in remarkable contrast with native Mb with a 6-coorinated NO−heme.[20] A minor amount of another 5-coordinated species can be observed at $g' = 2.10$. A three-lined hyperfine splitting pattern at g_z might be overlapped with that of the major component. In addition, a very small amount of a 6-coordinated species can be observed at high field extreme, as noted by the arrow at $g^{(6)} = 1.982$. Time-dependent observation indicated that the major species of the 5-coordinate structure of the NO complex of ferrous hemiporphycene Mb is stable for at least 3 h on ice.

Discussion

Reconstituted Protein. The 1:1 binding stoichiometry of ferric hemiporphycene with apoMb infers structural integrity of the resultant holoprotein. It is notable that the light absorption (Table 1) and EPR (Figure 4) spectra of the imidazole complex of the reconstituted Mb closely resemble those of the model compound, the bis(imidazole) derivative of ferric hemiporphycene. The spectral similarities are consistent with the F8-histidine being the proximal base in the reconstituted Mb. The visible absorption of ferric Mb in Figure 2 markedly changes with pH. The pH dependence demonstrates the presence of an iron-bound water molecule that dissociates into hydroxide at alkaline pH.[12c] These results demonstrate that the axial coordination structure of native Mb, i.e., ligation of the proximal histidine and a water molecule, is retained in iron hemiporphycene Mb as well. Furthermore, low-spin EPR signals of the ferric hemiporphycene Mb at 5 and 15 K bear close resemblance to those of the imidazole Mb and ferric hemiporphycene bis(imidazole) in organic solvent, as shown in Figure 4. This indicates that distal E7-histidine is forced partly to coordinate to the central iron due to a conformational transition on sample freezing at cryogenic temperature. The reversible oxygenation depicted in Figure 5 confirms the integrity of coordination structure for the iron hemiporphycene in Mb. Since apoMb incorporates etiohemin,[9] a hemin isomeric with the iron hemiporphycene, the coupling of apoMb with iron hemiporphycene is not surprising.

Functional Anomalies. One notable result for hemiporphycene Mb is the high O_2 affinity. There are several factors to cause the functional anomaly. One might state that the altered function comes from conformational change of globin residues after insertion of the hemiporphycene. This possibility may be ruled out because the normal acid−alkaline transition in Figure 2 suggests that the axial coordination environment including the proximal and distal histidines is almost unchanged. In addition, X-ray crystallography on the Mbs containing the iron complexes of porphine[21] or *meso*-tetraalkylporphyrins[22,23] demonstrates that molecular shape of the prosthetic group only slightly affects the globin side-chain conformations. It could be still argued that absence of propionate groups in hemiporphycene causes a high O_2 affinity. The possibility is also discarded because the Mbs containing alkyl hemes[24,25] without propionates exhibit normal O_2 binding. It is therefore likely that the altered function of hemiporphycene Mb comes not from the molecular periphery of prosthetic group but from the asymmetric metallo core in hemiporphycene.

Our preliminary expectation was that hemiporphycene Mb will exhibit lower O_2 and CO affinities in comparison with

(19) Li, T.; Quillin, M. L.; Phillips, G. N., Jr.; Olson, J. S. *Biochemistry* **1994**, *33*, 1433−1446.
(20) Palmer, G. In *Iron Porphyrins*; Lever, A. B. P., Gray, H. B., Eds.; Addison-Wesley: London, 1983; Part II, pp 43−88.
(21) Neya, S.; Funasaki, N.; Sato, T.; Igarashi, N.; Tanaka, N. *J. Biol. Chem.* **1993**, *268*, 8935−8942.
(22) Sato, T.; Tanaka, N.; Moriyama, H.; Matsumoto, O.; Takenaka, A.; Neya, S.; Funasaki, N. *Bull. Chem. Soc. Jpn.* **1992**, *65*, 739−745.
(23) Hata, T.; Hata, Y.; Sato, T.; Tanaka, N.; Neya, S.; Funasaki, N.; Katsube, Y. *Bull. Chem. Soc. Jpn.* **1991**, *64*, 821−828.
(24) Neya, S.; Funasaki, N.; Imai, K. *J. Biol. Chem.* **1988**, *263*, 8810−8815.
(25) Neya, S.; Funasaki, N.; Shiro, Y.; Iizuka, T.; Imai, K. *Biochim. Biophys. Acta* **1994**, *1208*, 31−37.

native Mb because the deformed metallo core could less favorably accommodate the displaced deoxy iron atom. Such an account has been proposed for corrphycene iron in a trapezoidal coordination cavity.[6] Contrary to the expectation, hemiporphycene Mb has a higher O_2 affinity by 12-fold than native Mb. It is also notable that the CO affinity is almost unchanged or rather slightly reduced. For these reasons, the ratio of the two equilibrium constants $K_{CO}/K_{O_2} = 1.7$ of ferrous hemiporphycene Mb is significantly smaller than $K_{CO}/K_{O_2} = 25$ of native Mb[17] and $K_{CO}/K_{O_2} = 15$ of mesoheme-Mb.[16] Our kinetic measurements affording $K_{CO}/K_{O_2} = 4.0$, which is larger than $K_{CO}/K_{O_2} = 1.7$, are still consistent with the decreased CO/O_2 discrimination in hemiporphycene-Mb. Since π-type of back-bonding interaction is important in the Fe(II)−CO bond,[26a] and since both σ- and π-type interactions contribute in the Fe(II)−O_2 bond,[5] the decreased K_{CO}/K_{O_2} value for hemiporphycene Mb suggests an enhanced σ-bonding character in the Fe(II)−O_2 bond. It appears in hemiporphycene Mb that changes in the axial Fe(II)−O_2 interaction dominate over those in the equatorial Fe−N(pyrrole) interactions.

The iron atom in hemiporphycene MbO_2 possesses "pseudooctahedral" symmetry. In this situation, the asymmetrically arrayed four equatorial nitrogen atoms destabilize the orthogonal $d_{x^2-y^2}$ lobe of iron. Destabilization of the $d_{x^2-y^2}$ orbital in turn lowers the energy level of the d_{z^2} orbital, as observed for octahedral transition-metal complexes upon Jahn−Teller distortion.[26b] The stabilized d_{z^2} orbital could make a more favorable overlap with the π^* orbital of O_2. In other words, a high O_2 affinity of hemiporphycene Mb comes from a stabilized d_{z^2} orbital of the iron in a distorted equatorial field. It follows that enhanced σ-bonding character of the Fe(II)−O_2 bond could slow O_2 dissociation from the Mb. This is in agreement with the results that the dissociation of O_2 is solely retarded while association rate is almost unchanged in ferrous hemiporphycene Mb.

Another notable observation of ferrous hemiporphycene Mb is that NO complex is dominantly 5-coordinate, as shown in Figure 7. The observation indicates that the geometric strain in the four equatorial bonds becomes apparent when a potential π-acceptor NO coordinates. The iron atom connected with four nonorthogonal equatorial bonds tends to be displaced more readily than that in the square porphyrin core. Strong Fe(II)−NO interaction causes partial rupture the iron−histidine bond as detected with EPR (Figure 7).

Heterogeneity of the Coordinating Ligands. The coordination structure of the iron-bound ligand in the reconstituted Mb is not homogeneous. The IR spectrum of the MbCO as shown in Figure 6 resolves three absorption bands, in contrast with the two main CO bands at 1945 and 1932 cm^{-1} in native Mb.[19] The band positions of 1958, 1942, and 1928 cm^{-1} are well within the ranges of 1965−1956 cm^{-1} (conformer A_0), 1936−1953 cm^{-1} (A_1 and A_2), and 1916−1932 (A_3) cm^{-1} reported for native and numerous mutant Mbs.[19] The three CO bands in ferrous hemiporphycene Mb are not necessarily correlated with the function because the kinetic trace of CO binding exhibits a single-exponential decay. This observation is in agreement with the proposal by Li et al.[19] that there is little direct correlation between CO stretching frequency and CO affinity. They further suggested that the multiple CO bands come from conformational variability that reflects the electrostatic potential difference in the distal heme pocket. If we follow their interpretation, the bound CO could adopt three dominant conformations with a comparable magnitude in ferrous hemiporphycene Mb. We note a similar observation for the CO in ferrous corrphycene Mb,[6a] where three IR bands are observed at 1970, 1952, and 1937 cm^{-1}. It is possible that electrostatic potential in the immediate vicinity of the iron-bound CO is influenced with modified ring-current field of the deformed porphyrin rings.

It is also notable that the ligand heterogeneity is resolved in ferric Mb as well.The EPR spectrum of the imidazole derivative in Figure 4 exhibits two low-spin species whereas the EPR of native Mb imidazole displays a single species.[27] Why does ferric hemiporphycene Mb exhibit heterogeneous EPR signals? The most probable cause is the asymmetric molecular shape of the prosthetic group. The axial Fe(III)−imidazole bond is not a C_4-symmetry axis in hemiporphycene. Under this circumstance, orientation of the imidazole ring sensitively affects the $p\pi-d\pi$ overlap with iron atom. It follows that the simple model compound without globin matrix could resolve two EPR species. This is indeed the case. The EPR spectrum of the bis(imidazole) complex in chloroform (part D, Figure 4) exhibits two ferric low-spin species with $g = 2.582$, 2.29, and 1.775 and $g = 2.471$, 2.29, and 1.825, respectively. Thus, iron hemiporphycene Mb exhibits ligand heterogeneities for the CO and imidazole derivatives. The characteristic results found for the ferrous and ferric derivatives are most likely to come from the distorted metallo core in hemiporphycene.

In summary, iron atoms acquire characteristic ligand-binding properties in hemiporphycene. Iron hemiporphycene in Mb enhances the O_2 binding ability and reveals the novel discrimination mechanism between O_2 and CO. In view of the functional anomalies induced by the iron complexes of hemiporphycene and corrphycene[6] in Mb, we conclude that the square metallo cavity in protoporphyrin is essential for the regular function of native Mb.

Acknowledgment. We thank Professor J. S. Sessler, University of Texas, as a reviewer and for informing us of his early attempt to reconstitute myoglobin with iron hemiporphycene.

IC020504T

(26) Shriver, D. F.; Atkins, P. W.; Langford, C. H. *Inorganic Chemistry*, 2nd ed.; Oxford University Press: Oxford, U.K., 1994; (a) pp 666−668, (b) pp 255−256

(27) Hori, H. *Biochim. Biophys. Acta* **1971**, *251*, 227−235.